

Strategy for automated analysis of passive microseismic data based on S-transform, Otsu's thresholding, and higher order statistics

G-Akis Tselentis¹, Nikolaos Martakis², Paraskevas Paraskevopoulos¹, Athanasios Lois², and Efthimios Sokos¹

ABSTRACT

Small-magnitude seismic events, either natural or induced microearthquakes, have increasingly been used in exploration seismology with applications ranging from hydrocarbon and geothermal reservoir exploration to high-resolution passive seismic tomography surveys. We developed an automated methodology for processing and analyzing continuously recorded, single-channel seismic data. This method comprised a chi-squared-based statistical test for microseismic event detection and denoising filtering in the S-transform domain based on the Otsu thresholding method. An automatic P-phase picker based on higher order statistics criteria was used. The method was used with data from a surface seismic station. The performance of the method was tested and evaluated on synthetic and real data from a microseismic network used in a high-resolution PST survey and revealed a high level of consistency.

station/receiver, detect microseismic events and their corresponding P-phase arrival times. The aim is processing a large number of continuous seismic records and producing accurate P-wave arrivals. To achieve this, three steps are followed. Initially, a detection algorithm is used to detect the parts of the recordings that could contain seismic events. Then these segments are cut and denoised in the S-transform domain. Finally, a more accurate P-wave arrival picker is applied. In this way, the segments of the records that contain potential events are identified quickly and the more computationally intensive parts of denoising and P-wave phase picking can be applied only to the selected segments of the records. For the multiple sensors that make up a recording network/array, the detection algorithm can be applied in parallel for each recording channel separately, giving us the possibility to exclude events detected by less than a preset number of stations (e.g., three or four). Also, the picking algorithm is run for each event for all stations that detected it. This enables us to have an estimate of the consistency of the automatic picking and knowing the geometry of the stations have an initial identification of the outliers. Because this method is applied at each processed channel separately, the recording configuration can be irregularly distributed.

INTRODUCTION

During enhanced hydrocarbon recovery operations such as hydraulic fracturing or during high-resolution passive seismic tomography (PST), small-magnitude earthquakes are used to increase our knowledge of reservoir characteristics.

As the stations recording in each survey increase in number and sampling frequency, data sets become too large for manual processing to be effective. Event detection and accurate arrival time picking from the recorded seismograms can be very hard due to the generally low signal-to-noise ratios (S/Ns) of the recorded events. In this paper, we present a strategy to automatically process continuous seismic records from a microseismic network or an array of receivers and, by processing one selected component for each

The induced seismic activity by hydraulic fracturing is used for improving hydrocarbon production (e.g., Maxwell and Urbancic, 2001; Eisner et al., 2006; Shapiro et al., 2006), in geothermal energy reservoir characterization (e.g., Norio et al., 2008), and monitoring CO₂ sequestration (e.g., Warpinski et al., 1999). Recently, the application of high-resolution PST surveys in regional hydrocarbon exploration has demonstrated that its resolution is strongly dependent on the number of seismological stations used (Tselentis et al., 2011a). Thus, for a conventional PST survey, we end up with a vast amount of seismic waveforms to process (Durham, 2003; Kapotas et al., 2003; Martakis et al., 2006; Tselentis et al., 2011).

For high-resolution PST applications, we need as many as possible of small magnitude events that can be considered as point sources. These small events, especially if acquired in areas of high

Manuscript received by the Editor 10 August 2011; revised manuscript received 17 April 2012; published online 18 September 2012.

¹University of Patras, Seismological Laboratory, Rio, Greece. E-mail: tselenti@upatras.gr; paris@geology.upatras.gr; esokos@upatras.gr.

²LandTech Enterprises, Athens, Greece. E-mail: nmartakis@landtechsa.com; lois@upatras.gr.

© 2012 Society of Exploration Geophysicists. All rights reserved.

anthropogenic activity, are often strongly affected by noise. The high noise level makes the accurate determination of P-wave arrival difficult, so procedures that allow a more reliable first arrival picking are required (Tselentis et al., 2011a).

DETECTION OF MICROSEISMIC EVENTS

Event detection is the initial step of this data processing flow. The seismic records, in addition to the seismic events of interest, contain noise with varying energy levels and frequency content that often mask these events. The records containing the events must be identified before any other processing can be applied. Most event-detection algorithms are based on computing the fluctuation of S/N as a function of time for a specified frequency band. The

Table 1. Common event-detection methodologies proposed in the literature.

Category	Authors
Maximum likelihood	Freiberger, 1963 Chung et al., 2001
Fractal	Tosi et al., 1999
Envelope	Allen, 1978 Stewart, 1977 Earle and Shearer, 1994
Waveform correlation	Gibbons and Ringdal, 2006 Arrowsmith and Eisner, 2006 Song et al., 2010 Hanafy et al., 2007 Eisner et al., 2008 Drew et al., 2005
Spectral density	Shensa, 1977
Walsh transform	Goforth and Herrin, 1981 Fletcher and Sharon, 1983 McGarr et al., 1964
Filtering	Clark et al., 1981 Sterns et al., 1981
Evolution spectra	Vincent et al., 2004
Particle motion	Wagner and Owens, 1996 Withers et al., 1999
Kalman filtering	Baziw and Weir-Jones, 2002
STA/LTA	Swindell and Snell, 1977 Houliston et al., 1984 Shamshi et al., 1990 Ruud and Husebye, 1992 Tong, 1995 Yung and Ikelle, 1997 Botella et al., 2003 Sharma et al., 2006 Kumar et al., 2009 Khadhraoui et al., 2010

most commonly used approach is the short- to long-term average ratio (STA/LTA) method. In this approach, the absolute values of the signal within a long and a short moving time window are summed and their ratio calculated. When the STA/LTA exceeds a user-defined threshold, a detection time for the recording receiver is assigned. This can be applied in either one of the components (usually the vertical one) or a combination of them. The details of this method can be found in Trnkoczy (2009). Many other event-detection methods have also been proposed by various researchers, and the most common are listed in Table 1.

In the present investigation, we follow a new, microseismic event-detection method, instead of STA/LTA. This method is based on the chi-squared-based statistical test under a sequential hypothesis testing framework.

The chi-squared goodness-of-fit test (also known as Karl Pearson's test) is often used to test the equivalence of a probability density function (PDF) of a measured data set against a theoretical one.

As usually applied, this test considers a set of N independent observations from a random variable x with a PDF, $p(x)$. The N observations are grouped into K equal frequency interval bins, forming a frequency histogram. A usual measure for the total discrepancy for all class intervals is the following parameter q (Bendat and Piersol, 1986):

$$q = \sum_{i=1}^K \frac{(O_i - E_i)^2}{E_i}, \quad (1)$$

where the number of observations falling within each class interval is called the observed frequency (O_i) and the number of the observations expected to fall within each bin is called the expected frequency (E_i).

For the case of a time series seismic signal, the distribution of the seismic noise is unknown; thus, using the equal length bins selection could falsely result in zero estimations for specific bins, which would drive q to infinity. This problem prompted us to apply a modified Pearson's test (Lois et al., 2010).

In our approach, the samples in the selected time window of the record are also used to estimate the expected frequencies. Instead of equal length bins, assuming that the seismic noise follows a known distribution we use an equal number of observations per bin, keeping the number of samples in each bin the same (equiprobable partitioning) while changing the lengths of the bins, and instead of the frequencies O_i and E_i , we use the corresponding lengths of the bins L_i^O and \hat{L}_i^E .

The L_i^O is calculated for every window of the continuous recording that we use from the equiprobable partitioning of the observed PDF, while \hat{L}_i^E is calculated before the analysis by selecting a noise segment of the record indicative of the noise, containing no bursts or earthquakes. If the continuous recording spans several days and the character of the seismic noise changes significantly during that time, a new \hat{L}_i^E could be recalculated.

Figure 1a shows a random signal window, its equal length bins partition (Figure 1b), and its equal number of observations per bin partitioning (Figure 1c) used in our approach. An obvious advantage is that we avoid having zero values; an example is the first bin of Figure 1b, for the equal length bins partition. We have also selected to use the natural logarithm of the calculated parameter for noise suppression purposes because it has proven to work better with the thresholding that is used subsequently. Thus, we introduce the following modified statistical test for the event detection:

$$q_m = \ln \left(\sum_{i=1}^K \frac{(L_i^O - \hat{L}_i^E)^2}{\hat{L}_i^E} \right). \quad (2)$$

In equation 2 for a sufficient number of bins, it is improbable that $L_i^O - \hat{L}_i^E = 0$ for all steps i . The proposed modification of the Pearson statistical test does not follow a X_{K-1}^2 distribution, and to solve the event-detection problem, we have designed a thresholding-type hypothesis testing framework using the Otsu method (Otsu, 1979) that provides an optimal separation between noise and seismic events. The flowchart in Figure 2 summarizes the various stages of the proposed event-detection methodology.

Obviously, the initial input is the continuous recording of the time series in which seismic events might or might not be present. Thus for given record X_n , $n = 1, 2, \dots, T$, we form an estimation of the PDF $f(x)$ of the test, by computing its values by means of a sliding window of length N . In this way, equation 2 can be written as

$$q_m(X_{n-N+1}^n) = \ln \left(\sum_{i=1}^K \frac{(L_i^O(X_{n-N+1}^n) - \hat{L}_i^E)^2}{\hat{L}_i^E} \right). \quad (3)$$

The window length is set empirically and can depend on the range of magnitudes of the events we are looking. For example, for the magnitudes in the real data set presented, a 1 s window was used. For smaller events that have small duration and rapid changes, a shorter window could be selected, while for larger events, a longer window could be selected.

As the window becomes bigger, the test curve becomes smoother, meaning a larger probability for missing an event. The smaller the window, the more sensitive it is to rapid changes but the more computing intensive. For selecting the number of observations per bin, we take into account two important restrictions. A large number of bins, with respect to the length of the used window, is needed to have high resolution for our analysis, but also based on Bendat and Piersol (1986), each nonequal-length bin must contain at least three samples (observations). For the type of events used on the synthetic example and the real test that follows, a window of 1 s (100 samples) was used. In our application, each bin consisted of five samples dividing the moving window into 20 nonequal-length bins.

The Otsu thresholding method will be applied on the calculated values of the parameter q_m . For any given value p , we can separate the values of the previously calculated chi-squared test into the following two classes:

$$\begin{aligned} C_0(p) &= \{q_m(X_{n-N+1}) \leq p\}, \\ C_1(p) &= \{q_m(X_{n-N+1}) > p\}. \end{aligned} \quad (4)$$

The goal of using this method in this stage is to find the optimal value p^* that will provide the optimal separation between the noise distribution

and the distribution of seismic events. Using these classes, $f(x)$ can be expressed as follows:

$$f(x) = \lambda_0(p)f_0(x; p) + \lambda_1(p)f_1(x; p), \quad (5)$$

where $f_i(x)$ is the PDF of the class $C_i(p)$, $i = 1, 2$, and $\lambda_i(p)$ the percentage of points belonging into each class. Following the thresholding scheme of Otsu (1979), we define the following cost function:

$$\sigma_B(p) = (\mu_1(p) - \mu_0(p))^2 \lambda_0(p) \lambda_1(p), \quad (6)$$

where $\mu_i(p)$ are the mean values of the class $C_i(p)$. Then, by finding the p value for which σ_B becomes maximum

$$p^* = \operatorname{argmax}_p \sigma_B(p), \quad (7)$$

we obtain an optimum separation of the classes, which is equivalent to solving the following hypothesis-testing problem. In this hypothesis testing, our initial assumption (H_0) is that the sliding window is comprised of noise. When our test exceeds the critical value p^* , calculated by the Otsu thresholding, this initial hypothesis is not valid and the alternative (H_1) is true, indicating the presence of a seismic event within the window

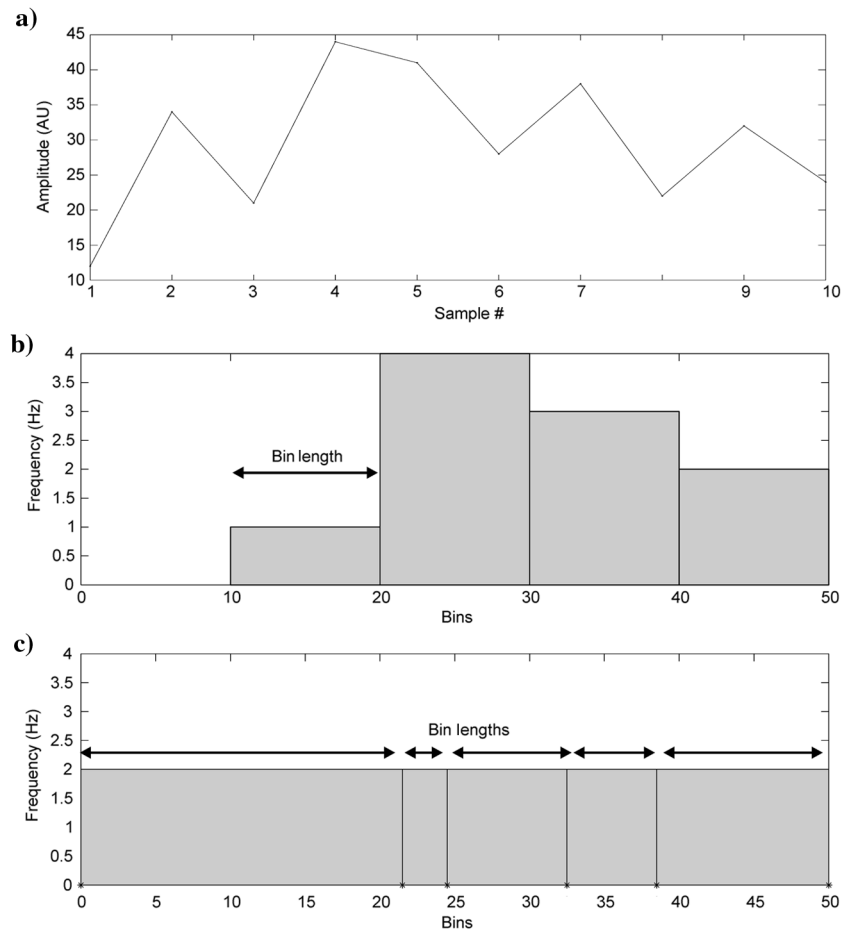


Figure 1. (a) Random signal, (b) its equal length bins partition, and (c) its equal number of observations per bin partitioning.

H_0 = noise process and $H_1 \neq$ noise process,

by deciding H_i if $q_m(X_{n-N+1}) \in C_i(p^*)$, $i = 1, 2$. In this way, the windows that we expect to contain seismic events are identified and will be used in the next processing stages.

DENOISING

The presence of seismic noise in the record can deteriorate the performance of the picking algorithms, especially in the case of small events. So an important step in the processing is to attenuate the energy of the seismic noise while not only preserving the energy from the event but also avoiding altering the arrival times of the seismic phase. Filtering methods are often used to suppress noise to improve the S/N. As the energy of the seismic noise present in the signal can have diverse characteristics a number of filtering techniques have been used for noise filtering. Some filtering methods commonly employed for seismic noise attenuation are listed in Table 2.

Geophysical data processing has adapted and used, techniques initially developed for image filtering (Ristau and Moon, 1997; Hale, 2001; Fehmers and Höcker, 2003; Ferahtia et al., 2009). Bad-dari et al. (2011) propose the anisotropic nonlinear diffusion filter initially used for image filtering (Perona and Malik, 1990) to reduce noise in seismic data.

A similar approach based on the S-transform is also applied successfully by Banister et al. (2010) to denoise microseismic data from a geothermal field. In the present paper, we have combined

the S-transform and the Otsu thresholding image processing criterion to automate the filtering process of noisy seismic records.

The calculation of the S-transform of the signal is the first step in denoising. The S-transform (Stockwell et al., 1996) is used to transform a signal in the time domain, producing a localized spectrum in the time-frequency domain. The S-transform of the signal $x(t)$ is given by the following equation:

$$S(\tau, f) = \int_{-\infty}^{\infty} x(t) \frac{|f|}{\sqrt{2\pi}} e^{-\frac{(t-\tau)^2 f^2}{2}} e^{-i2\pi f t} dt, \quad (8)$$

where t is time, f is frequency, and τ controls the position of the Gaussian window along the time axis.

An important property of the S-transform is its reversibility; that is, the initial signal $x(t)$ can be fully recovered from its transform $S(\tau, f)$. Simon et al. (2007) show that to recover the inverse S-transform, the following equation should be used, so that the creation of artifacts can be avoided:

$$x(t) = \sqrt{2\pi} \int_{-\infty}^{\infty} \frac{S(t, f)}{|f|} e^{i2\pi f t} df. \quad (9)$$

Another important property of the S-transform is its linearity, and for the case of additive noise to the signal, the data can be modeled as $\text{data}(t) = \text{signal}(t) + \text{noise}(t)$; thus, the S-transform can be written as

$$S\{\text{data}(t)\} = S\{\text{signal}(t)\} + S\{\text{noise}(t)\}. \quad (10)$$

To minimize the effect of noise, the Otsu thresholding method is applied once again on the signal but this time in the time-frequency domain. Initially, a histogram is constructed using the elements of the 2D matrix $S(\tau, f)$. As in the case of event selection, an optimal p^* value is searched that can separate the areas of the S-transform in two clusters: one dominated by the signal's high energy (higher amplitudes) and the other by noise. This procedure is applied twice: once for the real part and once for the imaginary part of the S-transform. This way, the filter designed has two components that are applied on the real and imaginary parts of the signal in the time-frequency domain. The result is inverse S-transformed,

Table 2. Commonly used noise reduction methodologies in seismic signals.

Category	Authors
Singular value decomposition	Ursin and Zheng, 1985 Lu, 2006
Principal component analysis	Hagen, 1982
Karhunen-Loève transform	Al-Yahya, 1991
Eigen image	Jones and Levy, 1987 Canales, 1984 Gulunay, 1986
Artificial neural networks	Essenreiter, 1999 Djarfour et al., 2008
Fuzzy methods	Hashemi et al., 2008

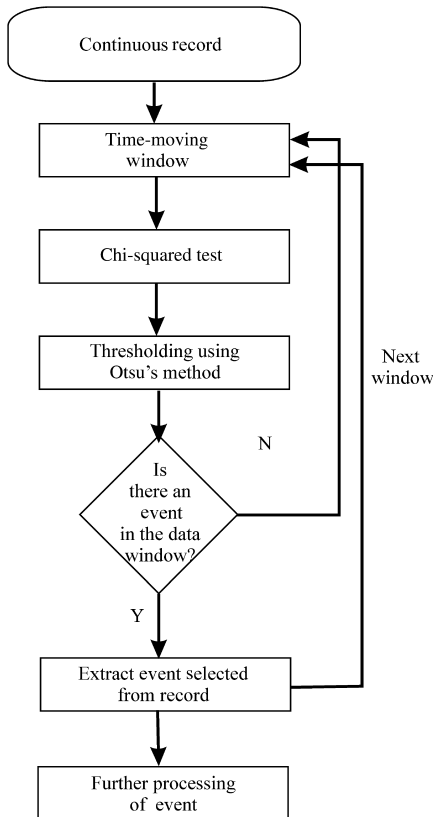


Figure 2. Event-detection algorithm flowchart.

to retrieve the filtered signal in the time domain. This method can clear the first arrival to improve the accuracy of the first pick in moderate to high S/Ns, but it will not work as well in a very low S/N in which the energy of the seismic noise is comparable to that of the seismic event. The next step of the processing flow is P-phase picking on the denoised signal.

P-PHASE PICKING

Accurate picking of P-wave arrival times is very important for reservoir monitoring or PST surveys. Accurate automatic event detection and picking, especially when dealing with large data sets, can speed up and help improve the quality of the picks. Various methodologies have been proposed, the most common of which are presented in Table 3. The method used in this paper is based on the properties of higher order statistics (HOS) parameters, namely, “skewness, kurtosis, and differential entropy” (also known as “negentropy”).

The first- and second-order statistics (such as mean value, variance, autocorrelation, and power spectrum) are extensively used in signal processing to describe linear and Gaussian processes. In practice, many processes deviate from linearity and Gaussianity. HOS can be used for the study of such processes (Nikias and Petropulu, 1993).

Let $\{X(k)\}$, $k = 1, 2, 3, \dots, M$ is a real stationary discrete time signal of length M , and its moments up to order 4 exist; the estimators used are

$$sk(X) = \frac{\sum_{i=1}^N \{(X(i) - \hat{m}_x)^3\}}{(N-1)\hat{\sigma}_x^3} \quad (11)$$

and

$$kur(X) = \frac{\sum_{i=1}^N \{(X(i) - \hat{m}_x)^4\}}{(N-1)\hat{\sigma}_x^4}, \quad (12)$$

where \hat{m}_x is the mean and $\hat{\sigma}_x$ the standard deviation of $\{X(k)\}$ and N is the length of the time-moving window that is used for the estimation (Saragiotis et al., 2002).

In the present study, we estimate the P-phase arrival time using these HOS parameters and, additionally, an estimation of the negentropy $J(X)$ defined as a function of skewness and kurtosis (Jones and Sibson, 1987)

$$J(X) \approx \frac{1}{24} sk^2(X) + \frac{1}{48} kur^2(X). \quad (13)$$

According to the implemented algorithm (Saragiotis et al., 2002), a moving window “slides” on the recorded signal, estimating skewness, kurtosis, and negentropy. Skewness can be considered as a measure of symmetry of the distribution, while kurtosis is a measure of heaviness of the tails, so they are suitable for detecting parts of the signal that do not follow the amplitude distribution of ambient noise. Seismic events have higher amplitudes in comparison to the seismic noise, and these higher values occupy the tails of the distribution (high degree of asymmetry of distribution). In the case of seismic events, skewness and kurtosis obtain high values, presenting maxima in the transition from ambient noise to the seismic

Table 3. P-phase picking methodologies.

Category	Authors
Energy ratio criteria (STA/LTA)	Swindell and Snell, 1977 Allen, 1978 Saari, 1991 Ruud and Husebye, 1992 Earle and Shearer, 1994 Baer and Kradolfer, 1987 Hildyard et al., 2008 Abaseyev, 2009
Autoregressive methods	Morita and Hamaguchi, 1984 Takanami and Kitagawa, 1988, 1991 Sleeman and Van Eck, 1999 Leonard and Kennett, 1999 Leonard, 2000
Fractal-based methods	Boschetti et al., 1996
Seismic polarity assumption	Flinn, 1965 Montalbetti and Kanasevich, 1970 Vidale, 1986 Jurkevics, 1988 Magoira et al., 1987, 1989 Cichowicz, 1993 Wagner and Owens, 1996 Anderson and Nehorai, 1996
Neural networks	Wang and Teng, 1995, 1997 Mousset et al., 1996 Dai and MacBeth, 1995, 1997 Zhao and Takano, 1999 Gentili and Mhelini, 2006
Maximum likelihood and high-order statistics methods	Christofferson et al., 1988 Roberts et al., 1989 Kushnir et al., 1990 Saragiotis et al., 2002, 2004
Fuzzy logic	Chu and Mendel, 1994
Wavelet transform	Anant and Dowla, 1997 Yung and Ikelle, 1997
Pattern recognition	Joswig, 1990
Hybrid methods	Saragiotis et al., 1999 Akazawa, 2004 Diehl et al., 2009

events (P-arrival). Out of the above criteria, kurtosis appears to perform better than the others (Lois et al., 2010; Tselentis et al., 2011a).

As the curves of these HOS parameters' are calculated using a sliding window in time, they reach their maximum values only when the time window contains a large fraction of energy from the seismic event beyond the P-arrival. So to have an accurate estimation of the P onset time, it is preferable to use the maximum

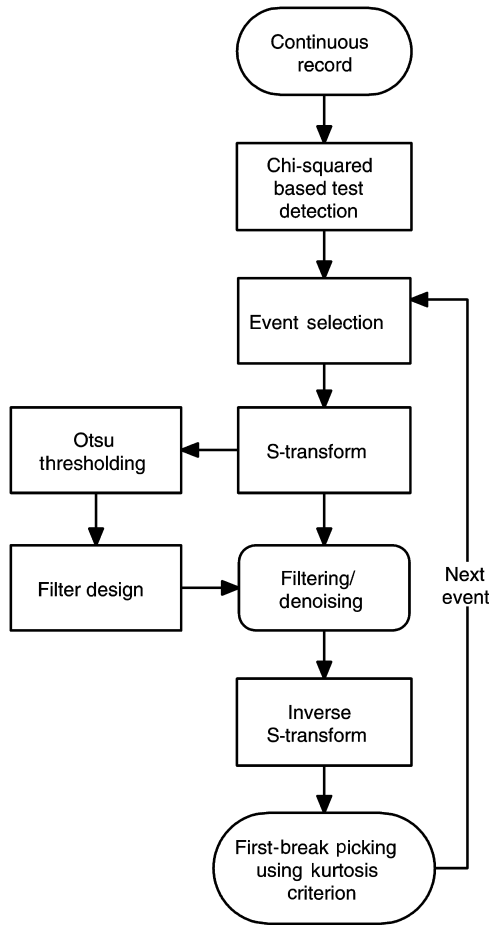


Figure 3. Flowchart of the proposed methodology for event detection, denoising, and P-phase picking.

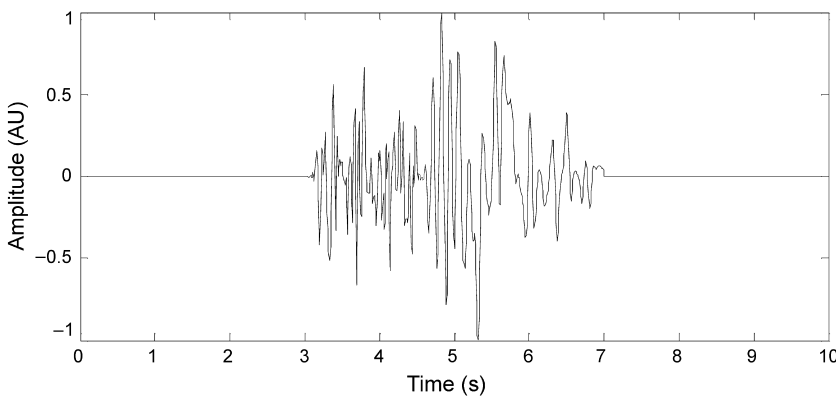


Figure 4. Noise-free synthetic signal.

slope and not the maximum values of these parameters. Figure 3 presents the stages of the proposed event-detection and P-phase picking methodology. It has been implemented in C++ code and requires minor computer resources when running on a conventional PC and processing the data in real time, even in the case of an array of several stations.

TESTS AND RESULTS

Application on synthetic data

Initially, the outlined methodology was extensively tested on synthetic data. The synthetic test consists of constructing a synthetic “eventlike” seismic record for which the accurate onset is known. Then we apply our method on this “event” and calculate the P-wave arrival time. This way we can compare the result of the method with an exact P-wave arrival time to better estimate the error. The synthetic seismograms were constructed by the following procedure: initially Gaussian noise is filtered with a Park-McClellan optimal equiripple finite impulse response filter. This is repeated two times. Initially, for keeping the P-frequencies from 20 up to 40 Hz and the second time for S-waves we keep frequencies from 10 to 15 Hz. Next, the signal is multiplied by a negative exponential function to simulate the effect of the P- and S-coda attenuation. The part of the signal corresponding to S-waves is shifted in time, and the two signals are added (Figure 4).

To introduce noise to the synthetic test, an appropriately scaled window with real noise from a seismic record can be added to the event that we want to detect. By using the standard deviations of the noise record and the synthetic event, the exact S/N can be calculated using

$$S/N = 20 \log_{10} \left(\frac{\sigma_{\text{signal}}}{\sigma_{\text{noise}}} \right). \quad (14)$$

Based on the S/N level we want to test, the amplitudes of the ambient noise are multiplied by the suitable scalar to scale to the desired amplitudes, before adding them to the synthetic event. Next, the chi-squared-based test statistic is applied to verify the existence of the event (Figure 5) and q_m is calculated using equation 3. The thick black line at amplitude 1 indicates the points of the record whose q_m values belongs to class C_1 (signal), while the black line indicates the record of the signal C_0 (noise). This test has shown that this method can detect the event sufficiently well. There is also a very short false detection after the end of the event, which we believe was caused by the way the synthetic event abruptly stops and the signal becomes flat again (Figure 4). We have tested this approach with various levels of noise with good results. With this procedure we have been able to detect events even in very noisy signals with S/Ns as low as 5 dB and in some test cases even lower.

The next step is to transform the seismic signal into the time-frequency domain by applying the S-transform. Using the Otsu thresholding method to the real and the imaginary part of the transform, the filter is automatically designed and applied. Finally, the onset of the first arrival is automatically picked using the HOS (in this case the kurtosis) criterion.

In Figure 6b, the effect of S-transform filtering can be seen on the noisy synthetic seismogram in Figure 6a. The automatic picking results using the kurtosis criterion to the unfiltered and filtered seismograms are also shown.

When comparing to the true pick, we can see that the picking accuracy for the filtered signal is improved versus the noisy one. The applied methodology has the additional advantage of not

altering the P-phase arrival. The whole process runs automatically without needing to fine-tune the parameters.

Application on real data

In this section, we test the proposed methodology on real data. A continuous noisy seismic record of 10 minutes. is selected, and the

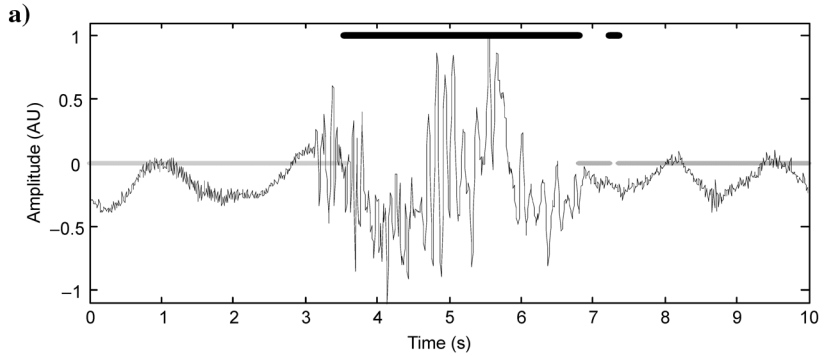


Figure 5. (a) Synthetic signal with addition of noise and the results from the chi-squared-based event detection. The thick black lines at value 1 indicate the detection of a seismic event, while the gray ones at zero indicate seismic noise. (b) Histogram of test q_m with the Otsu optimal threshold value.

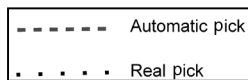
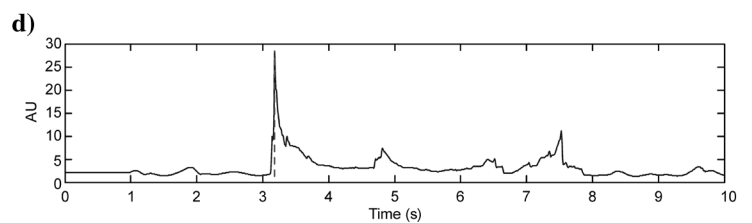
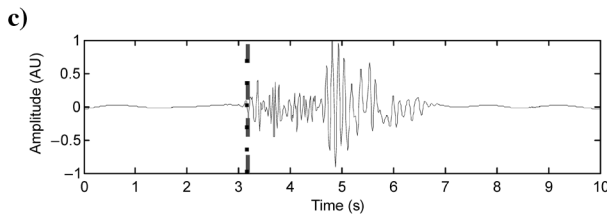
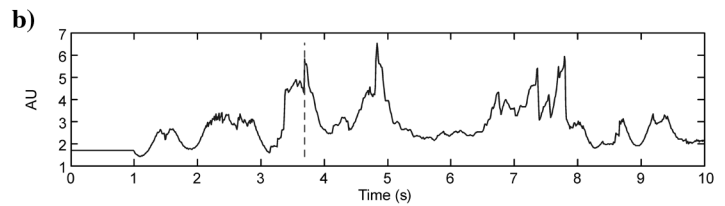
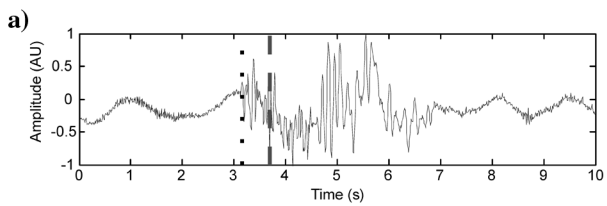
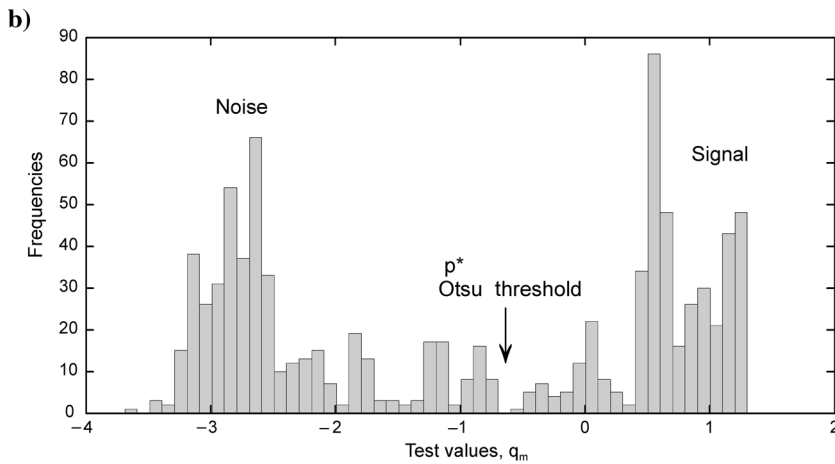


Figure 6. (a) Synthetic seismogram with addition of real seismic noise (b) Kurtosis calculated for the initial synthetic seismogram. (c) Seismogram filtered in the time-frequency domain using the S-transform. (d) Kurtosis calculated for the filtered synthetic seismogram. The dashed line is the automatic pick as calculated using the HOS (kurtosis) criterion, and the dotted line is the actual position of the P-phase arrival.

chi-squared-based test is applied (Figure 7). All five events in this record (A to E) were successfully detected. Also, there was a false detection on a record segment (F), which had higher amplitudes and different frequency content than the record noise, justifying the selection by the algorithm, but as can be seen in Figure 7, in contrast to the seismic events (A to E) its waveform is not typical of an earthquake (more simple) and secondarily it was not present in neighboring stations. Based on this it was found not to be a usable signal. From the detected events, we select one with a low S/N. Similar to the case of the synthetic data, the S-transform is applied on the signal (Figure 8) and the event is filtered by the designed filter based on the Otsu thresholding method. Finally, the first arrival is automatically picked using the kurtosis criterion.

A disadvantage of the method is that the HOS criteria when the level of noise is close to the level of the signal could miss the first arrival, picking a secondary one instead. Such a mispick can be seen in the noisy (raw) signal of Figure 7a. Here, denoising can reduce such mispicks improving the accuracy.

Figure 7. Section of real data recording. (A, B, C, D, E, and F indicate the parts of the signal that the algorithm identified as events.) Zoomed area shows event (A) selected to apply the proposed methodology. Vectors indicate the detected events; the thick black dots at approximately value one indicate the presence of seismic events as resulted from the proposed methodology.

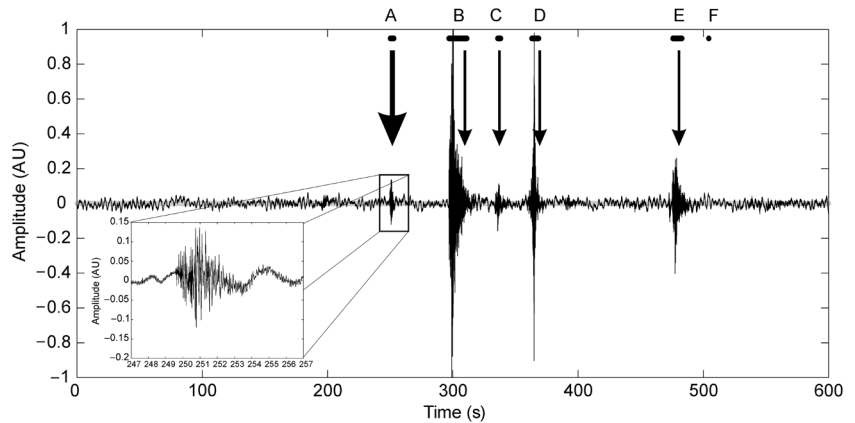


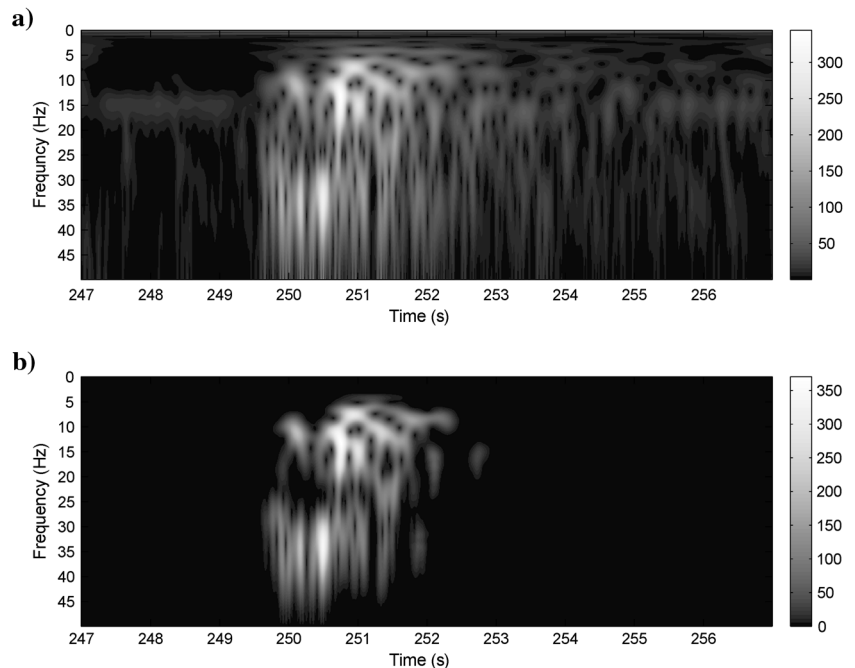
Figure 9a and 9b compares the automatic P-phase picking with the real one, for the unfiltered and filtered signal, respectively, showing a better agreement with the manual pick.

Application on multisensor real data

A characteristic of the events recorded in a microseismic network during a high-resolution PST survey is that their epicenters are inside or close to the network and they mostly have low magnitudes. To evaluate the performance of the above three HOS-based methods (skewness, kurtosis, and negentropy), 15 seismic events (Figure 10) were selected from a PST survey in a hydrocarbon field in southeast Albania (Tselentis et al., 2011a). These were recorded by a 50-station microseismic network using LandTech’s LT-S100 3C velocity sensors, with a sampling rate of 200 samples per second.

These events have magnitudes ranging from 1.1 to 1.8 ML, their energy is relatively low, and their depths range from 2.5 up to 11 km. All records, having a P-wave arrival picked by an expert analyst, were used (353 arrivals).

Figure 8. (a) S-transform of the selected event and (b) corresponding S-transform after application of the filter.



From each station’s continuous record after the detection algorithm has indicated the presence of a seismic event, a segment of the record that starts 5 s before the detection and ends 5 s after the end of the detection. This ensures that the seismic segment selected contains the seismic event. This processing can be executed in parallel for more than one station, decreasing the time needed. Finally, the results for all the stations of the network can be compared and the events detected in less than four stations disregarded as false.

The vertical components of these records were filtered using the previously described S-transform methodology. The three HOS-based picking algorithms were applied on the data set to compare their performance against each other, resulting in three sets of calculated automatic picks. Finally, the comparison of the automatic picks against the manual ones is used for calculating the residual times for measuring their performance.

The automatic P-phase onset identification is divided in two parts: a detection algorithm for locating segments of the record containing seismic events and an accurate picker (the automatic HOS). As a measure of the quality of the signal, we calculated the S/N for every event. To accomplish this, the standard deviation was calculated using a selected time window before the P-onset (noise) against the corresponding standard deviation for the window after it (signal and noise) using the following formula:

$$S/N = 20 \log_{10} \left(\frac{\sigma_{\text{signal+noise}}}{\sigma_{\text{noise}}} \right). \quad (15)$$

As can be seen, by examining the S/N versus the residual times (Figure 11), the quality of the picked times depends on the S/N of the record. In most cases, as the S/N increases the P-arrival times become quite accurate and with low residual times compared with the manually picked arrivals. On the other hand, as the S/N becomes lower the accuracy decreases, as the autopickers start missing the P-wave arrivals selecting either secondary arrivals or S-waves or noise bursts (e.g., anthropogenic noise, electronic noise) in the record.

The S/N was selected as a measure of the method’s performance, as the event’s magnitude is only indirectly correlated with the quality of the picks. For the same receiver hypocenter combination, a higher magnitude event will be more accurately picked, but a noisy receiver will perform worse than a quieter one for the same event.

We considered that data with residuals larger than 0.3 s have missed the P-wave arrival pulse and were ignored for the rest of the analysis. These missed arrivals were observed mainly in low S/Ns in which the noise could mask the real first arrival making the picking algorithm to select secondary P-arrivals or even the S-wave arrival. These criteria were fulfilled by about 85% of the picks (298 picks for skewness, 302 for kurtosis, and 301 for negentropy) and were subsequently used. It should be noted that about 81% of the picks (depending on the method) had residual times below 0.2 s. To visualize the residual times, we constructed the corresponding histograms (Figure 12). As can be seen, the residuals

are positive, as the window needs to slide and include a number of samples from the event before the HOS methods “register” the arrival. This effect can be minimized by finding a systematic delay and subtracting it. We have not done this, and we present the results as obtained (no artificial corrections were applied).

The mean values of the residuals for skewness, kurtosis, and negentropy are 0.0733, 0.0469, and 0.0559 s, respectively, with standard deviations at 0.0658, 0.0571, and 0.0638 s. Comparing the three sets of automatic picks, the kurtosis criterion provided marginally better results than the negentropy criterion and the skewness criterion had the least accurate results (Tselentis et al., 2011b).

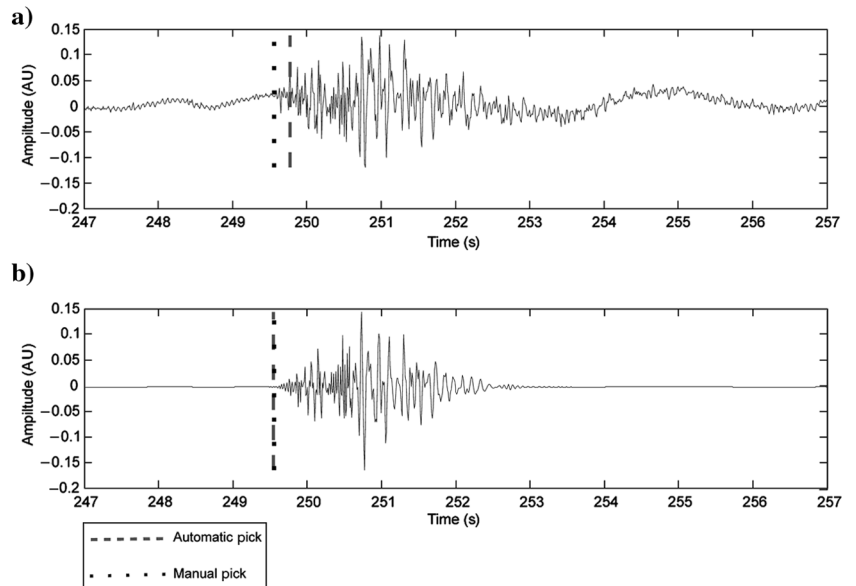


Figure 9. The event selected from (a) the real data and (b) those filtered in the time-frequency domain. The dashed line is the automatic pick as calculated using the HOS (kurtosis) criterion, and the dotted line is the actual position of the first break arrival.

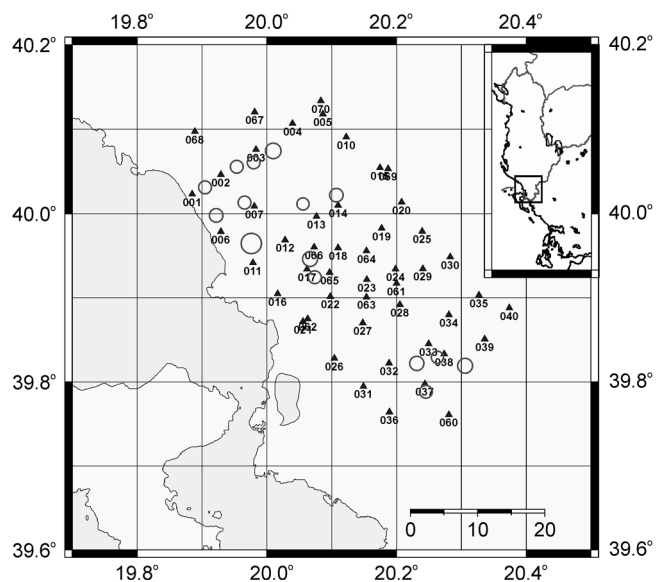


Figure 10. Seismological network (triangles) and microearthquakes (circles) used to test the proposed methodology.

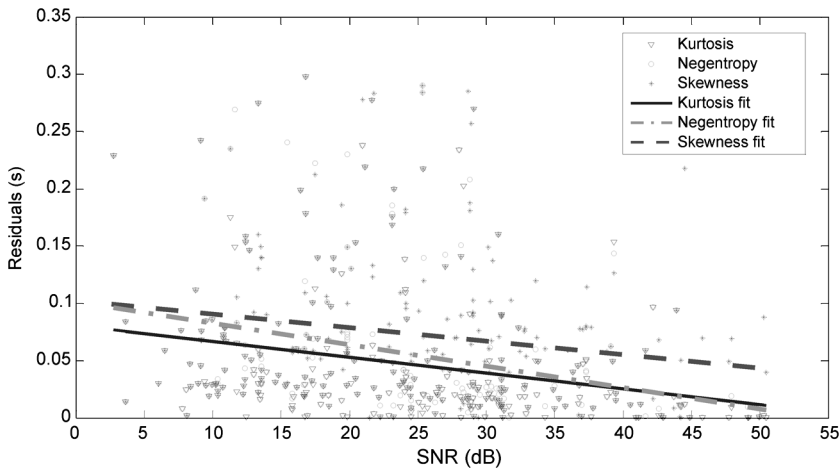


Figure 11. Diagram of S/N versus residual times for the three HOS parameters. The results are fitted with straight lines in a least-squares sense.

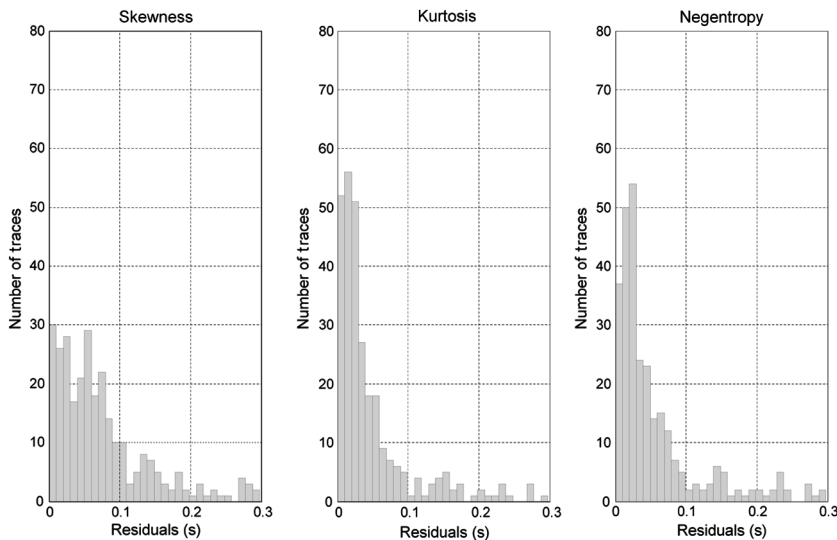


Figure 12. Histograms of the residuals for each of the HOS parameters.

CONCLUSIONS

We propose and apply an integrated method for seismic event detection, denoising, and accurate P-phase picking. The modified chi-squared test can be used for seismic events identification, requiring from the user only minimal parameter settings while making no assumptions about the distribution (e.g., Gaussian) of the seismic noise. The denoising of the events detected by the aforementioned algorithm takes place in the S-transform domain using the Otsu thresholding method. The S/N in the neighborhood of the P arrival can be improved, and this can help with the automatic estimation of the accurate P-phase arrival time using HOS criteria. In general this hybrid method is straightforward to implement and can be applied in parallel for a number of stations/receivers recording. Its advantages include the small number of parameters to be set requiring minimum user intervention after that and the ability to quickly

process large number of continuous seismic records and output relatively accurate first arrivals.

ACKNOWLEDGMENTS

We want to thank T. Nemeth, E. Slob, S. Maxwell, A. Rosca, and L. Eisner for their constructive comments that helped improve this paper. We also want to thank the personnel of the computer center of LandTech Enterprises for their help to implement the proposed methodology.

REFERENCES

- Abaseyev, S. S., M. Ammerman, and E. M. Chesnokov, 2009, Automated detection and location of hydrofracking-induced microseismic event from 3C observations in an offsetting monitor well: 79th Annual International Meeting, SEG, Expanded Abstracts, 1514–1518.
- Akazawa, T., 2004, A technique for automatic detection of onset time of P- and S-phases in strong motion records: *in* Proceedings of the 13th World Conference on Earthquake Engineering, International Association for Earthquake Engineering, paper no. 786.
- Allen, R. V., 1978, Automatic earthquake recognition and timing from single traces: *Bulletin of the Seismological Society of America*, **68**, 1521–1532.
- Al-Yahya, K. M., 1991, Application of the partial Karhunen-Loève transform to suppress random noise in seismic sections: *Geophysical Prospecting*, **39**, 77–93, doi: [10.1111/gpr.1991.tb00302.x](https://doi.org/10.1111/gpr.1991.tb00302.x).
- Anant, K. S., and F. U. Dowla, 1997, Wavelet transform methods for phase identification in three-component seismograms: *Bulletin of the Seismological Society of America*, **87**, 1598–1612.
- Anderson, S., and A. Nehorai, 1996, Analysis of polarized seismic wave model: *IEEE Transactions on Signal Processing*, **44**, 379–386, doi: [10.1109/78.485933](https://doi.org/10.1109/78.485933).
- Arrowsmith, S., and L. Eisner, 2006, A technique for identifying microseismic multiplets and application to the Valhall field, North Sea: *Geophysics*, **71**, no. 2, V31–V40, doi: [10.1190/1.2187804](https://doi.org/10.1190/1.2187804).
- Baddari, K., J. Ferahtia, T. Aifa, and N. Djarfour, 2011, Seismic noise attenuation by means of an anisotropic non-linear diffusion filter: *Computers and Geosciences*, **37**, 456–463, doi: [10.1016/j.cageo.2010.09.009](https://doi.org/10.1016/j.cageo.2010.09.009).
- Baer, M., and U. Kradolfer, 1987, An automatic phase picker for local and teleseismic events: *Bulletin of the Seismological Society of America*, **77**, 1437–1445.
- Banister, S., S. Sherburn, S. Bourguignon, S. Parolai, and D. Bowyer, 2010, Preprocessing for reservoir seismicity location: Rotokawa geothermal field, New Zealand: *in* Proceedings of the World Geothermal Congress 2010 Indonesia, International Geothermal Association, 201–205.
- Baziw, E., and I. Weir-Jones, 2002, Application of Kalman filtering techniques for microseismic event detection: *Pure and Applied Geophysics*, **159**, 449–471, doi: [10.1007/PL00001260](https://doi.org/10.1007/PL00001260).
- Bendat, J. S., and A. G. Piersol, 1986, *Random data, analysis and measurement procedures* (second ed.): Wiley-Interscience.
- Boschetti, F., M. Dentith, and R. List, 1996, A fractal-based algorithm for detecting first arrivals on seismic traces: *Geophysics*, **61**, 1095–1102.
- Botella, F., J. Rosa-Herranz, J. J. Giner, S. Molina, and J. J. Galiana-Merino, 2003, A real time earthquake detector with pre-filtering by wavelets: *Computers and Geosciences*, **29**, 911–919, doi: [10.1016/S0098-3004\(03\)00099-2](https://doi.org/10.1016/S0098-3004(03)00099-2).
- Canales, L. L., 1984, Random noise reduction: 54th Annual International Meeting, SEG, Expanded Abstracts, 525–527.
- Christofferson, A., E. S. Husebye, and S. F. Ingate, 1988, Wavelet decomposition using ML-probabilities in modelling single-site 3-component records: *Geophysical Journal*, **93**, 197–213, doi: [10.1111/gji.1988.93.issue-2](https://doi.org/10.1111/gji.1988.93.issue-2).

- Chu, C. K., and J. Mendel, 1994, First break refraction event picking using fuzzy logic systems: *IEEE Transactions on Fuzzy Systems*, **2**, 255–266, doi: [10.1109/91.324805](https://doi.org/10.1109/91.324805).
- Chung, P. J., M. L. Jost, and F. Bohme, 2001, Estimation of seismic wave parameters and signal detection using maximum likelihood methods: *Computers and Geosciences*, **27**, 147–156, doi: [10.1016/S0098-3004\(00\)00088-1](https://doi.org/10.1016/S0098-3004(00)00088-1).
- Cichowicz, A., 1993, An automatic S-phase picker: *Bulletin of the Seismological Society of America*, **83**, 180–189.
- Clark, A., G. Rogers, and W. Peter, 1981, Adaptive prediction applied to seismic event detection: *Proceedings of the IEEE*, **69**, 1166–1168, doi: [10.1109/PROC.1981.12140](https://doi.org/10.1109/PROC.1981.12140).
- Dai, H., and C. MacBeth, 1995, Automatic picking of seismic arrivals in local earthquake data using an artificial neural networks: *Geophysical Journal International*, **120**, 758–774, doi: [10.1111/j.1365-246X.1995.tb01851.x](https://doi.org/10.1111/j.1365-246X.1995.tb01851.x).
- Dai, H., and C. MacBeth, 1997, The application of back-propagation neural network to automatic picking seismic arrivals from single-component recordings: *Journal of Geophysical Research*, **102**, 15105–15113, doi: [10.1029/97JB00625](https://doi.org/10.1029/97JB00625).
- Diehl, T., E. Kissling, S. Husen, and F. Aldersons, 2009, Consistent phase picking for regional tomography models: Application to the greater alpine region: *Geophysical Journal International*, **176**, 542–554, doi: [10.1111/gji.2008.176.issue-2](https://doi.org/10.1111/gji.2008.176.issue-2).
- Djarfour, N., T. Aifa, K. Baddari, A. Mihoubi, and J. Ferahtia, 2008, Application of feedback connection artificial neural network to seismic data filtering: *Comptes Rendus Geoscience*, **340**, 335–344, doi: [10.1016/j.crte.2008.03.003](https://doi.org/10.1016/j.crte.2008.03.003).
- Drew, J., D. Leslie, P. Armstrong, and G. Michaud, 2005, Automated microseismic event detection and location by continuous spatial mapping: *Proceedings, in Proceedings of the Annual Technical Conference and Exhibition, SPE*, paper 95513-MS.
- Durham, L. S., 2003, Passive seismic. Listen: Is it the next big thing?: *AAPG Explorer*, **24**, 127–131.
- Earle, E. S., and E. M. Shearer, 1994, Characterization of global seismograms using an automatic-picking algorithm: *Bulletin of the Seismological Society of America*, **84**, 366–376.
- Eisner, L., D. Abbott, W. B. Barker, J. Lakings, and M. P. Thornton, 2008, Noise suppression for detection and location of microseismic events using a matched filter: 78th Annual International Meeting, SEG, Expanded Abstracts, 1431–1435.
- Eisner, L., T. Fischer, and J. Le Calvez, 2006, Detection of repeated hydraulic fracturing (out-of-zone growth) by microseismic monitoring: *The Leading Edge*, **25**, 547–554, doi: [10.1190/1.2202655](https://doi.org/10.1190/1.2202655).
- Essenreiter, R., 1999, Identification and attenuation of multiple reflections with neural networks: Ph.D. thesis, Universität Karlsruhe.
- Fehmers, G. C., and C. F. W. Höcker, 2003, Fast structural interpretation with structure-oriented filtering: *Geophysics*, **68**, 1286–1293, doi: [10.1190/1.1598121](https://doi.org/10.1190/1.1598121).
- Ferahtia, J., N. Djarfour, K. Baddari, and R. Guerin, 2009, Application of signal dependent rank-order mean filter to the removal of noise spikes from 2D electrical resistivity imaging data: *Near Surface Geophysics*, **7**, 159–169, doi: [10.3997/1873-0604.2009006](https://doi.org/10.3997/1873-0604.2009006).
- Flinn, E. A., 1965, Confidence regions and error determinations for seismic event location: *Reviews of Geophysics*, **3**, 157–185, doi: [10.1029/RG003i001p00157](https://doi.org/10.1029/RG003i001p00157).
- Freiberger, W., 1963, An approximate method in signal detection: *Quarterly of Applied Mathematics*, **20**, 373–378.
- Fretcher, K., and N. Sharon, 1983, Walsh transforms in seismic-event detection: *IEEE Transactions on Electromagnetic Compatibility*, **EMC-25**, 367–369, doi: [10.1109/TEMC.1983.304101](https://doi.org/10.1109/TEMC.1983.304101).
- Gentili, S., and A. Michelini, 2006, Automatic picking of P and S phases using a neural tree: *Journal of Seismology*, **10**, 39–63, doi: [10.1007/s10950-006-2296-6](https://doi.org/10.1007/s10950-006-2296-6).
- Gibbons, S. J., and F. Ringdal, 2006, The detection of low magnitude seismic events using array-based waveform correlation: *Geophysical Journal International*, **165**, 149–166, doi: [10.1111/gji.2006.165.issue-1](https://doi.org/10.1111/gji.2006.165.issue-1).
- Goforth, T., and E. Herrin, 1981, An automatic seismic signal detection algorithm based on the Walsh transform: *Bulletin of the Seismological Society of America*, **71**, 1351–1360.
- Gulunay, N., 1986, FXDECON and complex Wiener prediction filter: 56th Annual International Meeting, SEG, Expanded Abstracts, 279–281.
- Hagen, D. C., 1982, The application of principal components analysis to seismic data sets: *Geoexploration: International Journal of Mining and Technical Geophysics and Related Subjects*, **20**, 93–111, doi: [10.1016/0016-7142\(82\)90009-6](https://doi.org/10.1016/0016-7142(82)90009-6).
- Hale, D., 2001, Atomic images — A method for meshing digital images: *Proceedings of the 10th International Meshing Roundtable*, Sandia National Laboratories, 185–196.
- Hanafy, S. M., W. Cao, L. McCarter, and G. T. Schuster, 2007, Locating trapped miners using time-reversal mirrors: *Utah tomography and modelling/migration development project, annual report*, 11–24.
- Hashemi, H., A. Javaherian, and R. Babuska, 2008, A semi-supervised method to detect seismic random noise with fuzzy GK clustering: *Journal of Geophysics and Engineering*, **5**, 457–468, doi: [10.1088/1742-2132/5/4/009](https://doi.org/10.1088/1742-2132/5/4/009).
- Hildyard, M. W., S. E. J. Nippres, and A. Rietbrock, 2008, Event detection and phase picking using a time-domain estimate of predominance period T^{pd} : *Bulletin of the Seismological Society of America*, **98**, 3025–3032, doi: [10.1785/0120070272](https://doi.org/10.1785/0120070272).
- Houliston, D. J., G. Waugh, and J. Laughlin, 1984, Automatic real time event detection for seismic networks: *Computers and Geosciences*, **10**, 431–436, doi: [10.1016/0098-3004\(84\)90043-8](https://doi.org/10.1016/0098-3004(84)90043-8).
- Jones, I. F., and S. Levy, 1987, Signal-to-noise ratio enhancement in multi-channel seismic data via the Karhunen-Loève transform: *Geophysical Prospecting*, **35**, 12–32, doi: [10.1111/j.1365-2478.1987.tb00800.x](https://doi.org/10.1111/j.1365-2478.1987.tb00800.x).
- Jones, M. C., and R. Sibson, 1987, What is projection pursuit?: *Journal of the Royal Statistical Society Series A*, **150**, 1–37, doi: [10.2307/2981662](https://doi.org/10.2307/2981662).
- Joswig, M., 1990, Pattern recognition for earthquake detection: *Bulletin of the Seismological Society of America*, **80**, 170–186.
- Jurkevics, A., 1988, Polarization analysis of three-component array data: *Bulletin of the Seismological Society of America*, **78**, 1725–1743.
- Kapotas, S., G.-A. Tselentis, and N. Martakis, 2003, Case study in NW Greece of passive seismic tomography: A new tool for hydrocarbon exploration: *First Break*, **21**, 37–42, doi: [10.3997/1365-2397.2003021](https://doi.org/10.3997/1365-2397.2003021).
- Khadhraoui, B., D. Leslie, J. Drew, and R. Jones, 2010, Real-time detection and localization of microseismic events: 80th Annual International Meeting, SEG, Expanded Abstracts, 2146–2150.
- Kumar, S., B. K. Sharma, P. Sharma, and M. A. Shamshi, 2009, 24 bit seismic processor for analyzing extra large dynamic range signals for early warnings: *Journal of Scientific and Industrial Research*, **68**, 372–378.
- Kushnir, A., V. Lapshin, V. Pinsky, and J. Fyen, 1990, Statistically optimal event detection using small array data: *Bulletin of the Seismological Society of America*, **80**, 1934–1950, doi: [10.1785/0120000026](https://doi.org/10.1785/0120000026).
- Leonard, M., 2000, Comparison of manual and automatic onset time picking: *Bulletin of the Seismological Society of America*, **90**, 1384–1390, doi: [10.1785/0120000026](https://doi.org/10.1785/0120000026).
- Leonard, M., and B. L. N. Kennett, 1999, Multi-component autoregressive techniques for the analysis of seismograms: *Physics of the Earth and Planetary Interiors*, **113**, 247–263, doi: [10.1016/S0031-9201\(99\)00054-0](https://doi.org/10.1016/S0031-9201(99)00054-0).
- Lois, A., E. Z. Psarakis, V. Pikoulis, E. Sokos, and G.-A. Tselentis, 2010, A new chi-squared based test statistic for the detection of seismic events and HOS based pickers' evaluation: Presented at the 32nd ESC Assembly.
- Lu, W., 2006, Adaptive noise attenuation of seismic images based on singular value decomposition and texture direction detection: *Journal of Geophysics and Engineering*, **3**, 28–34, doi: [10.1088/1742-2132/3/1/004](https://doi.org/10.1088/1742-2132/3/1/004).
- Magotra, N., N. Ahmed, and E. Chael, 1987, Seismic event detection and source location using single-station (three-component) data: *Bulletin of the Seismological Society of America*, **77**, 958–971.
- Magotra, N., N. Ahmed, and E. Chael, 1989, Single-station seismic event detection and location: *IEEE Transactions on Geoscience and Remote Sensing*, **27**, 15–23, doi: [10.1109/36.20270](https://doi.org/10.1109/36.20270).
- Martakis, N., S. Kapotas, and G.-A. Tselentis, 2006, Integrated passive seismic acquisition and methodology: Case studies: *Geophysical Prospecting*, **54**, 829–847, doi: [10.1111/gpr.2006.00584.x](https://doi.org/10.1111/gpr.2006.00584.x).
- Maxwell, S., and T. Urbancic, 2001, The role of passive microseismic monitoring in the instrumented oil field: *The Leading Edge*, **20**, 636–639, doi: [10.1190/1.1439012](https://doi.org/10.1190/1.1439012).
- McGarr, A., R. Hofmann, and G. Hair, 1964, A moving-time-window signal-spectra process: *Geophysics*, **29**, 212–220, doi: [10.1190/1.1439352](https://doi.org/10.1190/1.1439352).
- Montalbetti, J. F., and E. R. Kanawewich, 1970, Enhancement of teleseismic body phases with a polarization filter: *Geophysical Journal of the Royal Astronomical Society*, **21**, 119–129, doi: [10.1111/gji.1970.21.issue-2](https://doi.org/10.1111/gji.1970.21.issue-2).
- Morita, Y., and H. Hamaguchi, 1984, Automatic detection of onset time of seismic waves and its confidence interval using autoregressive model fitting: *Zisin*, **37**, 281–293.
- Mouset, E., Y. Cansi, R. Crusem, and Y. Souchet, 1996, A connectionist approach for automatic labelling of regional seismic phases using a vertical component seismogram: *Geophysical Research Letters*, **23**, 681–684, doi: [10.1029/95GL03811](https://doi.org/10.1029/95GL03811).
- Nikias, Ch. L., and A. M. Petropulu, 1993, Higher-order spectra analysis: A nonlinear signal processing framework: PTR Prentice-Hall.
- Norio, T., T. Yamaguchi, and G. Zylvoloski, 2008, The hijiori hot dry rock test site, Japan evaluation and optimization of heat extraction from a 2-layered reservoir: *Geothermics*, **37**, 19–52, doi: [10.1016/j.geothermics.2007.11.002](https://doi.org/10.1016/j.geothermics.2007.11.002).
- Otsu, N., 1979, A threshold selection method from gray-level histograms: *IEEE Transactions on Systems, Man and Cybernetics*, **9**, 62–66, doi: [10.1109/TSMC.1979.4310076](https://doi.org/10.1109/TSMC.1979.4310076).
- Perona, P., and J. Malik, 1990, Scale-space and edge detection using anisotropic diffusion: *IEEE Transactions on Pattern Analysis and Machine Intelligence*, **12**, 629–639, doi: [10.1109/34.56205](https://doi.org/10.1109/34.56205).

- Ristau, J. P., and W. M. Moon, 1997, Adaptive filtering of random noise in 2D geophysical data: *Journal of the Korean Society of Remote Sensing*, **13**, 191–202.
- Roberts, R. G., A. Christofferson, and F. Cassidy, 1989, Real-time event detection, phase identification and source location estimation using single station three-component seismic data: *Geophysical Journal International*, **97**, 471–480, doi: [10.1111/j.1365-246X.1989.tb00517.x](https://doi.org/10.1111/j.1365-246X.1989.tb00517.x).
- Ruud, B., and E. Husebye, 1992, A new three-component detector and automatic single-station bulletin production: *Bulletin of the Seismological Society of America*, **82**, 221–237.
- Saari, J., 1991, Automated phase picker and source location algorithms for local distances using a single three-component seismic station: *Tectonophysics*, **189**, 307–315, doi: [10.1016/0040-1951\(91\)90503-K](https://doi.org/10.1016/0040-1951(91)90503-K).
- Saragiotis, C., L. Hadjileontiadis, and S. Panas, 1999, A higher-order statistics-based phase identification of three-component seismograms in a redundant wavelet transform domain: *in Proceedings of the IEEE Workshop on Higher Order Statistics*, IEEE, 396–399.
- Saragiotis, C., L. Hadjileontiadis, I. Rekanos, and S. Panas, 2004, Automatic P phase picking using maximum kurtosis and κ -statistics criteria: *IEEE Transactions on Geoscience and Remote Sensing Letters*, **1**, 147–151, doi: [10.1109/LGRS.2004.828915](https://doi.org/10.1109/LGRS.2004.828915).
- Saragiotis, C. D., L. J. Hadjileontiadis, and S. M. Panas, 2002, PAI-S/K: A robust automatic seismic P phase arrival identification scheme: *IEEE Transactions on Geoscience and Remote Sensing*, **40**, 1395–1404, doi: [10.1109/TGRS.2002.800438](https://doi.org/10.1109/TGRS.2002.800438).
- Shamshi, M. A., B. K. Sharma, and S. K. Mittal, 1990, Microprocessor based digital cassette seismograph: *IETE Technical Review*, **7**, 66–69.
- Shapiro, S. A., C. Dinske, and E. Rothert, 2006, Hydraulic fracturing controlled dynamics of microseismic clouds: *Geophysical Research Letters*, **33**, L14312–L14315, doi: [10.1029/2006GL026365](https://doi.org/10.1029/2006GL026365).
- Sharma, B. K., S. Kumar, S. K. Mittal, and M. A. Shamshi, 2006, Design improvements in digital seismograph for recording long duration seismic events and aftershocks: *Journal of Scientific and Industrial Research*, **65**, 36–41.
- Shensa, M., 1977, The deflection detector, its theory and evaluation on short period seismic data: TR-77-03, Texas Instruments.
- Simon, C., S. Ventosa, M. Schimmel, A. Heldring, J. J. Dañobeitia, J. Gallart, and A. Manuel, 2007, The S-transform and its inverses: Side effects of discretizing and filtering: *IEEE Transactions on Signal Processing*, **55**, 4928–4937, doi: [10.1109/TSP.2007.897893](https://doi.org/10.1109/TSP.2007.897893).
- Sleeman, R., and T. Van Eck, 1999, Robust automatic p-phase picking: An on-line implementation in the analysis of broadband seismogram recordings: *Physics of the Earth and Planetary Interiors*, **113**, 265–275, doi: [10.1016/S0031-9201\(99\)00007-2](https://doi.org/10.1016/S0031-9201(99)00007-2).
- Song, F., H. S. Kuleli, M. F. Toksöz, E. Ay, and H. Zhang, 2010, An improved method for hydrofracture-induced microseismic event detection and phase picking: *Geophysics*, **75**, no. 6, A47–A52, doi: [10.1190/1.3484716](https://doi.org/10.1190/1.3484716).
- Stearns, D., S. Vortman, and J. Luke, 1981, Seismic event detection using adaptive predictors: *in IEEE International Conference on Acoustics, Speech and Signal Processing*, Vol. 3, IEEE, 1058–1061.
- Stewart, S., 1977, Real time detection and location of local seismic events in central California: *Bulletin of the Seismological Society of America*, **67**, 433–452.
- Stockwell, R. G., L. Mansinha, and R. P. Lowe, 1996, Localization of the complex spectrum: the S transform: *IEEE Transactions on Signal Processing*, **44**, 998–1001, doi: [10.1109/78.492555](https://doi.org/10.1109/78.492555).
- Swindell, W. H., and N. S. Snell, 1977, Station processor automatic signal detection system, phase I: Final report, station processor software development: Texas Instruments report no. ALEX(01)-R-77-01, AFTAC Contract Number F08606-76-C-0025, Texas Instruments, Inc.
- Takanami, T., and G. Kitagawa, 1988, A new efficient procedure for the estimation of onset times of seismic waves: *Journal of Physics of the Earth*, **36**, 267–290, doi: [10.4294/jpe1952.36.267](https://doi.org/10.4294/jpe1952.36.267).
- Takanami, T., and G. Kitagawa, 1991, Estimation of the arrival times of seismic waves by multivariate time series models: *Annals of the Institute of Statistical Mathematics*, **43**, 407–433, doi: [10.1007/BF00053364](https://doi.org/10.1007/BF00053364).
- Tong, C., 1995, Characterization of seismic phases — An automatic analyser for seismograms: *Geophysical Journal International*, **123**, 937–947, doi: [10.1111/gji.1995.123.issue-3](https://doi.org/10.1111/gji.1995.123.issue-3).
- Tosi, P., S. Barba, V. De Rubeis, and F. Di Luccio, 1999, Seismic signal detection by fractal dimension analysis: *Bulletin of the Seismological Society of America*, **89**, 970–977.
- Trnkoczy, A., 2009, Understanding and parameter setting of STA/LTA trigger algorithm, *in P. Bormann, ed., New manual of seismological observatory practice: IASPEI*, 1–20, e-book.
- Tselentis, G.-A., N. Martakis, P. Paraskevopoulos, E. Sokos, and A. Lois, 2011a, High-resolution passive seismic tomography (PST) for 3D velocity, Poisson's ratio ν , and P-wave quality Q_p in the Delvina hydrocarbon field, southern Albania: *Geophysics*, **76**, no. 3, B1–B24, doi: [10.1190/1.3560016](https://doi.org/10.1190/1.3560016).
- Tselentis, G.-A., P. Paraskevopoulos, A. Lois, and N. Martakis, 2011b, Higher order statistics based Pickers' evaluation, using data from a microseismic network: Presented at the Third Passive Seismic Workshop.
- Ursin, B., and Y. Zheng, 1985, Identification of seismic reflections using singular value decomposition: *Geophysical Prospecting*, **33**, 773–799, doi: [10.1111/gpr.1985.tb00778.x](https://doi.org/10.1111/gpr.1985.tb00778.x).
- Vidale, J. E., 1986, Complex polarization analysis of particle motion: *Bulletin of the Seismological Society of America*, **76**, 1393–1405.
- Vincent, W. P., L. F. Fogel, and D. B. Fogel, 2004, Using evolutionary computation for seismic signal detection. A homeland security application: Presented at the IEEE International Conference on Computational Intelligence for Homeland Security and Personal Safety, 62–66.
- Wagner, G., and T. Owens, 1996, Signal detection using multi-channel seismic data: *Bulletin of the Seismological Society of America*, **86**, 221–231.
- Wang, J., and T. Teng, 1995, Artificial neural network-based seismic detector: *Bulletin of the Seismological Society of America*, **85**, 308–319.
- Wang, J., and T. Teng, 1997, Identification and picking of S phase using an artificial neural network: *Bulletin of the Seismological Society of America*, **87**, 1140–1149.
- Warpinski, N., T. Branagan, K. Mahrer, S. Wolhart, and Z. Moschovidis, 1999, Microseismic monitoring of the mounds drill cuttings injection tests: *in Proceedings of the U.S. Symposium on Rock Mechanics*, **37**, 1025–1032.
- Withers, M., R. Aster, and C. Young, 1999, An automated local and regional seismic event detection and location system using waveform correlation: *Bulletin of the Seismological Society of America*, **89**, 657–669.
- Yung, S. K., and L. T. Ikelle, 1997, An example of seismic time picking by third-order bicoherence: *Geophysics*, **62**, 1947–1951, doi: [10.1190/1.1444295](https://doi.org/10.1190/1.1444295).
- Zhao, Y., and K. Takano, 1999, An artificial neural network approach for broadband seismic phase picking: *Bulletin of the Seismological Society of America*, **89**, 670–680.